Iranian Journal of Pharmaceutical Sciences
2025: 21 (1): 323-343
https://journals.sbmu.ac.ir/IJPS

Research Article

OPEN ACCESS

# Identification and Screening of Bioactive Phytocompounds against Matrix Metalloproteinase-9, Targeting Cancer Cell Proliferation and Angiogenesis

Faiqua Haque[a], Bisma Showkat[a], Khalid Rasheed[b], Imran Ansari[c], Varsha Pawar[d], Mudassir Alam[e*], G.G.H.A. Shadab[a]

[a] *Department of Zoology, Faculty of Life Sciences, Aligarh Muslim University, Aligarh 202002, India.*
[b] *Institute for Biochemistry, FB 08, Justus Liebig University, Heinrich-Buff-Ring 17, D-35392 Giessen, Germany.*
[c] *Department of Plant Tissue Culture, Sachdev Tissue Culture Lab, Damoh, Madhya Pradesh 470661, India.*
[d] *Community health centre, Barhi, Katni, Madhya Pradesh, 483770, India.*
[e] *Department of Biological Sciences, Indian Biological Sciences and Research Institute (IBRI), Noida, 201301, India.*

**Received:** April 23, 2025 **Last Revision:** June 07, 2025 **Accepted:** June 10, 2025 **Available online:** July 28, 2025.

**Abstract**

Matrix metalloproteinase-9 (MMP-9) is a zinc-dependent endopeptidase that plays a key role in tumor progression, metastasis, and angiogenesis by degrading extracellular matrix components and modulating cell signaling pathways. Due to its overexpression in various cancers and contribution to tumor microenvironment remodeling, MMP-9 is a critical therapeutic target for cancer therapy. This study employed a comprehensive computational strategy to identify natural MMP-9 inhibitors from phytochemical databases. Different bioinformatics methods, such as molecular docking, ADME/T profiling, PASS analysis, pIC50 analysis, drug-likeness prediction, and molecular dynamic (MD) simulation, were carried out. Molecular docking analysis revealed strong binding affinities for Naringenin (-9.5 kcal/mol) and Rhamnetin (-8.9 kcal/mol), which formed stable interactions with MMP-9's catalytic domain. PASS analysis further validated their inhibitory potential (Naringenin: Pa = 0.764; Rhamnetin: Pa = 0.755). Crucially, both compounds exhibited exceptional ADME/T properties, such as high oral bioavailability, optimal metabolic stability, and low toxicity risks, which are essential for preclinical drug development. The molecular dynamics simulations confirmed their binding stability, with favorable hydrogen bonding patterns and minimal structural fluctuations. Other promising candidates like Epigallocatechin-gallate, Naringenin, and Rhamnetin emerged as beautiful leads due to their dual advantages of potent MMP-9 inhibition and drug-like pharmacokinetic profiles. The findings support advancing these phytochemicals into experimental studies as potential anti-cancer agents targeting MMP-9-mediated pathological processes in cancer development.

*Keywords*: ADME/T; MMP-9; Molecular docking; MD simulation; Phytochemicals; Tumor.

## 1. Introduction

Cancer is the fastest-growing disease across the globe, with a record of 12 million people diagnosed with cancer each year. In developed countries, cancer has become a leading cause of death, and in developing countries, it is the second leading cause of death after heart disease.

*** Corresponding Author**:
**Mudassir Alam**, Department of Biological Sciences, Indian Biological Sciences and Research Institute (IBRI), Noida, 201301, India. E-mail: syedalamalig@gmail.com.

**Cite this article as**: Haque F., Showkat B., Rasheed Kh., Ansari I., Pawar V., Alam M., Shadab G.G.H.A. Identification and Screening of Bioactive Phytocompounds against Matrix Metalloproteinase-9, Targeting Cancer Cell Proliferation and Angiogenesis. Iran. J. Pharm. Sci., 2025, 21 (1): 323-343.

DOI: https://doi.org/10.22037/ijps.v21i1.48139

According to research, there will be 21 million new cancer diagnoses globally by 2030, with 17 million cancer-related deaths and 75 million cancer-diagnosed individuals annually [1]. Cancer progression refers to the series of stages a normal cell undergoes to become a malignant, invasive tumor cell. This process is typically characterized by a series of genetic mutations that confer advantages to the cells, enabling them to grow uncontrollably, evade cell death, and acquire the ability to invade surrounding tissues. The concept of "hallmarks of cancer," introduced by Hanahan and Weinberg, describes the fundamental capabilities that cancer cells acquire during progression [2]. These hallmarks include sustaining proliferative signaling, evading growth suppressors, resisting cell death, and inducing angiogenesis. As cancer cells progress, they not only acquire the ability to sustain themselves through constant signaling for growth and evade normal regulatory mechanisms, but they also gain the ability to spread beyond their original site [3]. Metastasis is the process by which cancer cells spread from the primary tumor to distant organs. This is the major cause of death in cancer patients and involves several stages [4], i.e., Invasion, Intravasation, Circulation, Extravasation, Colonisation, Growth in Distant Sites, and Angiogenesis in metastasis [5]. Extracellular matrix (ECM) remodeling plays a pivotal role in cancer progression, influencing key aspects such as tumor growth, invasion, metastasis, and response to therapy. The ECM provides structural support to tissues and serves as a dynamic environment that regulates cellular behaviour [6]. In cancer, the ECM undergoes significant alterations, which promote malignant characteristics and contribute to the aggressive nature of tumors**.** The ECM consists of a complex network of proteins, including collagens, fibronectin, laminin, elastin, and proteoglycans, as well as signaling molecules like growth factors and cytokines [7]. In normal tissues, the ECM maintains tissue architecture and homeostasis. However, during cancer progression, the ECM undergoes remodeling, which is driven by both cancer cells and stromal cells, such as fibroblasts, endothelial cells, and immune cells. ECM remodeling involves the synthesis, degradation, and modification of ECM components, leading to changes in tissue stiffness, architecture, and composition [8]. This remodeling is regulated by various proteases, primarily matrix metalloproteinases (MMPs), disintegrins, and disintegrin and metalloproteinase (ADAM) proteins [9].

MMPs are a family of zinc-dependent endopeptidases that play a central role in the degradation of the ECM. These enzymes are critical for the remodeling of the ECM, which is essential for normal physiological processes such as embryogenesis, wound healing, and tissue repair. However, in cancer, MMPs are dysregulated, contributing to pathological processes, including tumor progression, invasion, metastasis, and angiogenesis [10]. MMPs break down the ECM by cleaving various components, including collagens, elastin, fibronectin, and proteoglycans, allowing tumor cells to invade surrounding tissues and migrate to distant organs. As zinc-dependent endopeptidases, MMPs require a zinc ion at their catalytic site for enzymatic activity. This metal ion is essential for the hydrolysis of peptide bonds in ECM components, which results in the breakdown of the ECM architecture [11]. MMPs play an essential role in cancer metastasis by facilitating the degradation of ECM components, allowing tumor cells to invade the surrounding tissue, enter the bloodstream, and establish secondary tumors in distant organs [12]. Collagenases like MMP-1 degrade interstitial collagen, one of the major structural proteins of the ECM, while gelatinases like MMP-2 and MMP-9 degrade denatured collagen [13]. Matrix Metalloproteinase-9 (MMP-9), also known as type IV collagenase or gelatinase B, is one of the most studied members of the MMP family. It is a zinc-dependent endopeptidase primarily involved in the degradation of interstitial collagen, one of the most abundant and structurally important components of the ECM [14]. MMP-9 plays a pivotal role in tissue remodeling and is closely associated with tumor invasion, metastasis, and the overall progression of cancer [15]. MMP-9 cleaves collagen into smaller fragments by hydrolyzing the peptide bonds between specific glycine-proline motifs in the collagen molecule. This degradation process breaks down the ECM's structural framework, enabling tumor cells to invade surrounding tissues and migrate through the ECM [16]. It has been reported that MMP-9 also facilitates intravasation, a process by which cancer cells enter the bloodstream or lymphatic vessels [17]. By degrading the collagen-rich ECM at the invasive front of the tumor, MMP-9 enables cancer cells to breach tissue barriers and

reach vasculature. MMP-9 contributes to angiogenesis by remodeling the ECM around blood vessels, facilitating endothelial cell migration, and forming new capillaries [18].

Medicinal plants are a rich source of diverse bioactive compounds with significant therapeutic properties. Their medicinal potential has been extensively studied for centuries. These plants exhibit various pharmacological effects, including anti-inflammatory, antiviral, antitumor, antimalarial, and analgesic properties [19]. The chemical constituents found in medicinal plants predominantly exhibit antioxidant properties, contributing to their anti-cancer potential. The key bioactive compounds responsible for this antioxidant activity include flavones, isoflavones, flavonoids, anthocyanins, coumarins, lignans, catechins, and isocatechins [20]. The significant advantage of plant-derived compounds in cancer treatment and prevention lies in their safety, affordability, and ease of oral administration. However, some plant-based compounds may cause side effects, which can generally be managed through proper dosage control. These side effects do not diminish their relevance in phytochemical research [21]. Conventional cancer treatments such as chemotherapy and radiotherapy are costly and often associated with severe side effects, including myelosuppression, as well as neurological, cardiac, pulmonary, and renal toxicity, all of which significantly impact the patient's quality of life [22]. In recent years, there has been a growing scientific interest in exploring medicinal plants as a valuable source of potential anti-cancer agents.

Plant-based natural products have been an excellent source of new drug discovery over the past decades [23, 24]. However, using plant-derived compounds in cancer treatment dates back to the 1950s. Some of the earliest plant-based anti-cancer agents include vinca alkaloids such as vinblastine and vincristine and cytotoxic podophyllotoxins. Multiple reports confirm that several plant-derived anti-cancer drugs have progressed to clinical trials [25]. Among the significant milestones in these trials are flavopiridol, extracted from the Indian tree *Dysoxylum binectariferum*, and meisoindigo, obtained from the Chinese plant *Indigofera tinctoria*. These compounds have demonstrated lower toxicity than traditional chemotherapy drugs [26]. Study indicates that approximately 60% of available anti-cancer drugs are plant-based.

In many countries, medicinal plants are widely considered a viable alternative for cancer treatment [27]. Extensive cytotoxic screening of various plant species has been conducted to evaluate their anti-cancer properties and explore their potential for drug development [28]. Given the promising benefits of plant-derived anti-cancer drugs, their global use has steadily increased from 10% to 40%, with usage in Asia reaching as high as 50% [29]. The therapeutic potential of natural plant compounds highlights the necessity for further scientific screening and clinical trials to develop improved cancer treatment options. For over forty years, research has consistently highlighted the importance of extracellular matrix-remodeling enzymes, particularly MMPs, in modifying the tumor microenvironment during cancer progression [30]. MMP-driven ECM degradation not only promotes tumor invasion but also alters tumor cell behavior, leading to metastasis and disease progression. Therefore, inhibiting MMP activity is a promising therapeutic strategy for combating cancer [31]. Due to their involvement in cancer progression, they are considered valuable diagnostic and prognostic biomarkers for different cancer types and stages. Natural compounds have gained recognition as potential candidates in cancer research, offering a vast reservoir of bioactive molecules with therapeutic potential. Among these, flavonoids have attracted considerable interest due to their significant biological properties [32]. Their diverse mechanisms of action make them promising agents for extensive investigation in cancer therapy [33]. Diverse arrays of bioactive metabolites such as bioflavonoids, anthocyanins, carotenoids, and polyphenols have been demonstrated to exert synergistic effects by interacting with multiple molecular targets. These targeted approaches have strengthened research efforts to utilize natural products for therapeutic interventions in cancer and various pathophysiological disorders, where MMP-9 serves as a key regulatory factor [34]. Identifying and characterizing diverse natural plant-derived inhibitors hold significant potential in developing therapeutic agents. Novel plant-based natural inhibitors with an expanding understanding of MMP biology may enhance the prospects of successful translational applications.

## 2. Material and methods

### *2.1. Ligand retrieval and preparation*

The phytochemicals were obtained from Dr. Duke's Phytochemical and Ethnobotanical databases. The databases describe species, phytochemicals, biological functions, and ethnobotanical uses. The current Phytochemical and Ethnobotanical databases facilitate inquiries about plants, chemicals, bioactivity, and ethnobotany. Numerous plants and their chemical compositions are included, and the details are structured to enhance browsing and searching in multiple user-friendly ways [35].

The search term "anti-cancer" produced phytochemicals with corresponding properties. The chosen phytochemicals and their molecular weight (MW) and PubChem ID are listed in **table 1**. Only those phytochemicals were chosen from the database whose 3D SDF file was available on PubChem. Additionally, the SDF files for the ligands were obtained from the PubChem database [36]. The ligand was prepared using UCSF Chimera 1.15 [37]. The ligands' energy minimization was performed using the "structure editing" feature. The minimization parameters were configured to default settings, and the AMBER ff14SB force field was utilized with the Gasteiger charge [38].

### *2.2. Retrieval of target protein structure and its preparation*

The crystal structure of the target protein, Matrix metalloproteinase-9 (MMP-9), was obtained from the protein data bank (PDB) in PDB file format with ID 1GKC. The protein structure was prepared for molecular docking using Pymol 3.0 [39]. The hydroxamate (HETATOM) bound structure that acts as an inhibitor was eliminated from the active site. Additionally, water molecules were eliminated, and polar hydrogens were incorporated into the protein structure.

### *2.3. Virtual screening of the selected phytochemicals against a target protein*

Molecular docking of the chosen phytochemicals against MMP-9 was conducted using Autodock Vina [40], which is integrated within PyRx [41]. The protein structure was uploaded and transformed into a macromolecule. Additionally, the prepared phytochemical files were transformed into pdbqt file format utilizing OpenBabel [42] to ensure they were executable. The docking grid box was configured to dimensions of 52.25×21.24×129.55 Å, centered at 52.25, 44.93, and 74.40. The default exhaustiveness was established at 8.

**Table 1.** Phytochemicals chosen from Dr. Duke's Phytochemical and Ethnobotanical database with their molecular weight (MW) and PubChem ID.

| Chemical name | MW (g/mol) | ID |
|---|---|---|
| (-)-Epigallocatechin-gallate | 458.4 | 65064 |
| 10-hydroxycamptothecin | 364.4 | 97226 |
| Allamandin | 308.28 | 5281540 |
| Allixin | 226.27s | 86374 |
| Alpha-carotene | 536.9 | 6419725 |
| Alpha-terpineol | 154.25 | 17100 |
| Ar-turmerone | 216.32 | 160512 |
| Arctiin | 534.6 | 100528 |
| Aristolochic-acid | 341.27 | 2236 |
| Berberastine | 352.4 | 442180 |
| Berberine | 336.4 | 2353 |
| Brusatol | 520.5 | 73432 |
| Butyric-acid | 88.11 | 264 |
| Caffeic-acid | 180.16 | 689043 |
| Citral | 152.23 | 638011 |
| Cleomiscosin-a | 386.4 | 442510 |
| Corytuberine | 327.4 | 160500 |
| Curcumenol | 234.33 | 167812 |
| Curcumin | 368.4 | 969516 |
| Daidzein | 254.24 | 5281708 |
| Diosmin | 608.5 | 5281613 |
| Elemene | 204.35 | 6918391 |
| Enterodiol | 302.4 | 115089 |
| Enterolactone | 298.3 | 10685477 |
| Etoposide | 588.6 | 36462 |
| Falcarinol | 244.37 | 5281149 |
| Isoharringtonine | 531.6 | 73492 |
| Lignin | 509.4 | 175586 |
| Limonene | 136.23 | 22311 |
| Naringenin | 272.25 | 439246 |
| Neohesperidin | 610.6 | 442439 |
| Resveratrol | 228.4 | 445154 |
| Rhamnetin | 316.26 | 5281691 |
| S-allyl-l-cysteine | 161.22 | 9793905 |
| S-allylmercaptocysteine | 193.3 | 9794159 |
| Trans-3,5,4'-trihydroxystilbene | 444.8 | 91745415 |
| Vicenin-2 | 594.5 | 442664 |
| Batimastat* | 477.6 | 5362422 |
| Marimastat* | 331.41 | 119031 |

* reference drugs

### *2.4. Prediction of biological activity of the phytochemicals*

The biological activity of the selected phytochemicals was assessed using the Way2Drug PASS webserver [43]. The phytochemicals were assessed for their "MMP-9 inhibitor" activity. This is a comprehensive tool for assessing the biological activity spectrum for compounds.

### *2.5. Physiochemical properties of the phytochemicals*

The phytochemicals' physiochemical characteristics were evaluated using ADMETLAB 3.0 [44]. It offers a detailed understanding of the compounds' preclinical effectiveness and efficiently conducts calculations and predictions of plant's physicochemical properties.

### *2.6. Drug-likeness property of the phytochemicals*

The drug-likeness characteristics of the phytochemicals were clarified according to Lipinski's rule of 5 [45]. The Supercomputing Facility for Bioinformatics and Computational Biology (scfbio-iitd) server was utilized to assess the drug-likeness of the compounds according to the previously mentioned rule. The drug-likeness characteristic of the compounds was additionally confirmed through the Molsoft server [46].

### *2.7. pIC50 value prediction of phytochemicals*

A pIC50 value denotes the negative logarithm of a drug's IC50 value expressed in molar concentration. It functions as a standardized measure of medication strength. The pIC50 values of the chosen phytochemicals were determined using the CODD-Pred server [47].

### *2.8. ADME/T profile of the phytochemicals*

The absorption, distribution, metabolism, excretion, and toxicity (ADME/T) analysis was conducted utilizing the Deep-PK and Protox-III server [48]. The ADME/T evaluation thoroughly explains a compound's preclinical effectiveness and safety [49].

### *2.9. Molecular dynamic simulation*

A molecular dynamics (MD) simulation evaluated the ligand's binding stability at the target protein's active site. It was conducted utilizing the WebGro server offered by the University of Arkansas for Medical Sciences (https://simlab.uams.edu/) [50]. The GROMOS96 43A1 forcefield was utilized, and the Simple Point Charge (SPC) water model was applied. The chosen salt type was NaCl at a concentration of 0.15M. To minimize energy, the steepest descent integrator was employed for 5000 steps. The NVT/NPT equilibration method was applied, with the temperature fixed at 300K and the pressure maintained at 1 bar. The simulation was conducted for 50ns, with the number of frames per simulation set to 1000. MD simulation generated root mean square deviation (RMSD), root mean square fluctuation (RMSF), radius of gyration (Rg), solvent-accessible surface area (SASA), and the count of hydrogen bonds. These parameters assist in understanding the conformational changes and stability of the protein-ligand complexes [51].

### *2.10. Visualization of interaction between the phytochemicals and the target protein*

The two-dimensional and three-dimensional depiction of the protein-ligand interaction was conducted using Discovery Studio 2021, a comprehensive platform for molecular modeling, visualization, and analysis [52].

## 3. Results and discussion

### *3.1. Virtual screening of the phytochemicals*

The molecular docking study yielded docking scores for the phytochemicals with the target protein. Phytochemicals with docking scores less than -8 kcal/mol are depicted in **figure 1.** The docking score is important for analyzing the ligands' binding affinity with the protein's active site. The lower the docking score, the higher the binding affinity. **Figure 1** shows that D-delta-tocotrienol has the lowest docking scores among all phytochemicals, followed by betulinic acid. It implies that they show a strong affinity with the binding site of the MMP-9. Among the compounds, diosmin shows the most promising binding affinity with a score of -9.9, followed closely by naringenin (-9.5) and cleomiscosin-A (-9.4). Other notable high-affinity binders include Neohesperidin (-9.2), alpha-carotene (-9.2), arctiin (-9.1), daidzein (-9.1), and enterodiol (-9.1). Rhamnetin, with a score of -8.9, demonstrates binding potential comparable to resveratrol (-8.9) and stronger than compounds like enterolactone (-8.7) or vicenin-2 (-8.8).

Moderate binders include curcumin (-8.5), (-)-epigallocatechin-gallate (-8.2), and Ar-turmerone (-8.2), while berberastine (-8.0) and 10-hydroxy camptothecin (-8.7) exhibit relatively weaker interactions. Furthermore, we used batimastat (-6.8) and marimastat (-6.5) as reference drugs to compare the docking score of the phytochemicals. All phytochemicals showed better docking scores in comparison to the reference drugs. These computational results suggest that these phytochemicals may serve as strong MMP-9 inhibitors, warranting further experimental validation for therapeutic applications.

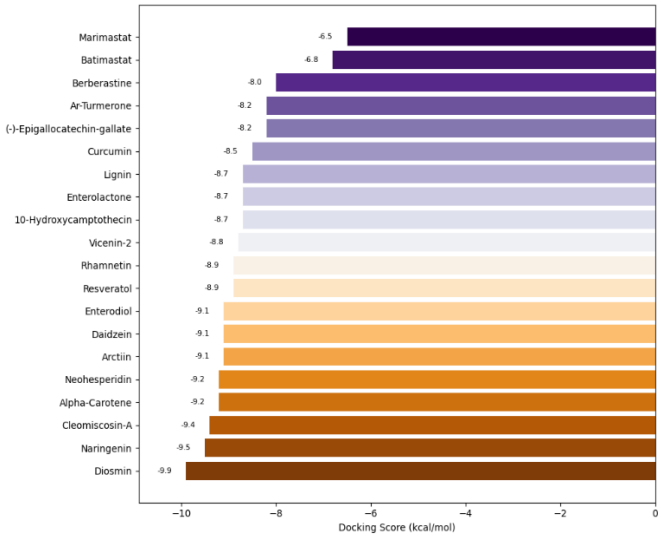


**Figure 1.** Molecular docking scores (kcal/mol) of the phytochemicals, marimastat, and batimastat as reference drugs.

### *3.2. PASS analysis*

The above-mentioned phytochemicals were analyzed for their MMP-9 inhibitor activity using PASS analysis. **Figure 2** provides analysis data evaluating the potential of various chemical compounds to act as MMP-9 inhibitors. The table lists each chemical name and two key probability values: Pa (Probability of Activity) and Pi (Probability of Inactivity). Compounds with higher Pa values (closer to 1) are more likely to exhibit inhibitory activity against MMP-9, while those with higher Pi values (closer to 1) are more likely to be inactive. For instance, Daidzein (Pa = 0.864, Pi = 0.002) and Alpha-Carotene (Pa = 0.883, Pi = 0.002) show strong potential as MMP9 inhibitors due to their high Pa and low Pi values. Conversely, Arctiin (Pa = 0.209, Pi = 0.192) has a lower likelihood of activity. Notable compounds with promising MMP9 inhibition potential include rhamnetin (Pa = 0.755), resveratrol (Pa = 0.772), and naringenin (Pa = 0.764). These results suggest that certain polyphenols and flavonoids may be particularly effective. The analysis is a predictive tool for identifying candidate molecules for further experimental validation as MMP-9 inhibitors, which are relevant in conditions like cancer and inflammation.

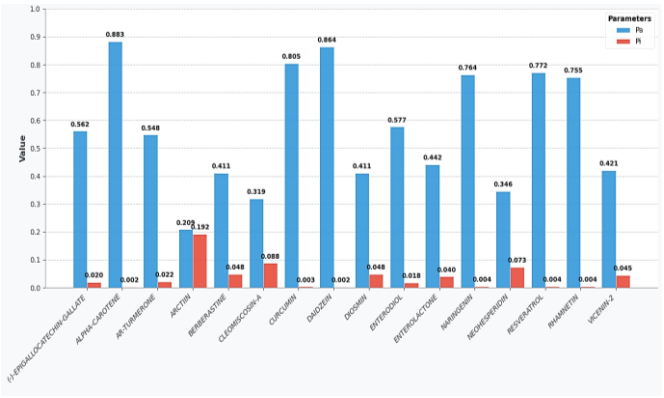


**Figure 2.** Pa (Probability of Activity) and Pi (Probability of Inactivity) of the selected phytochemicals for being MMP-9 inhibitors as evaluated by the PASS server.

### *3.3. pIC$_{50}$ value prediction of phytochemicals*

The pIC$_{50}$ value aids in evaluating the biological strength of a substance, particularly the capacity to hinder a biological process or target by 50%. It is represented as the minus logarithm of the IC50 measurement. This indicates that higher pIC50 values demonstrate increased potency. The biological or drug potency of the phytochemicals against MMP-9 was predicted using a CODD-PRED [53] server. **Figure 3** provides pIC50 values of various phytochemicals. For instance, Enterodiol has the highest PIC50 value (6.14), making it the most potent inhibitor in the list, followed by Lignin (5.48) and (-)-Epigallocatechin-gallate (EGCG) (5.65). Among the highlighted compounds, Rhamnetin (5.19) also demonstrates strong inhibitory activity, while Neohesperidin (4.71), Naringenin (4.67), and Diosmin (4.61) exhibit moderate but still notable effects. Arctiin (4.38) and Cleomiscosin-A (4.43) show relatively weaker potency at the lower end.

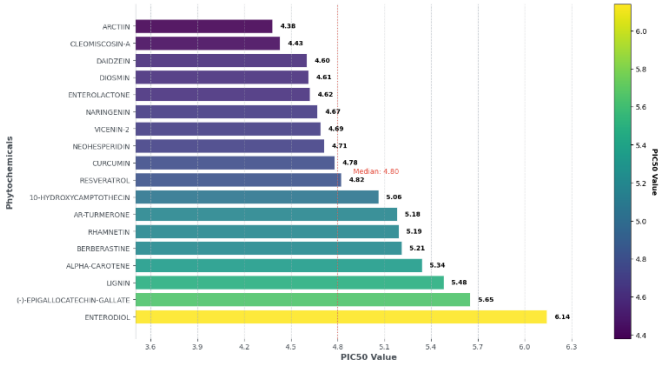


**Figure 3.** $pIC_{50}$ values of the phytochemicals as predicted by the CODD-PRED server.

### *3.4. Drug-likeness property of the phytochemicals*

The drug-likeness of the phytochemicals was assessed using a Molsoft server (**Figure 4**).

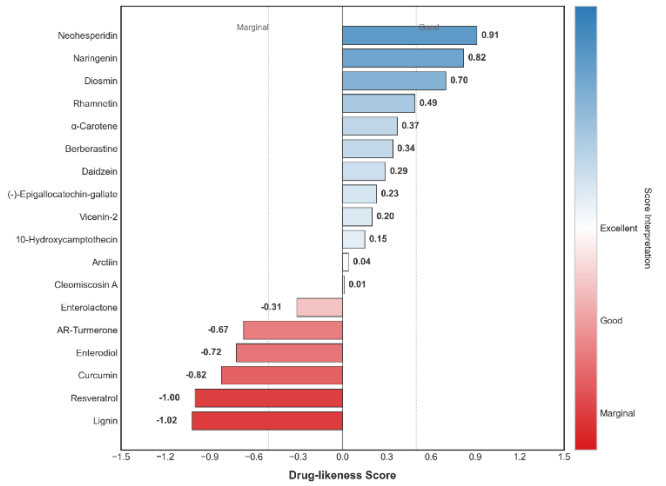


**Figure 4.** A drug-likeness score of the phytochemicals as evaluated by the Molsoft server.

A higher positive score generally suggests better drug-like properties, such as good absorption, distribution, metabolism, and excretion (ADME) profiles. In contrast, negative scores may indicate less favorable characteristics for drug development. For instance, compounds like Neohesperidin (0.91), Naringenin (0.82), and Diosmin (0.70) have relatively high positive scores, implying strong drug-like potential. On the other hand, compounds such as Lignin (-1.02), Resveratrol (-1.00), and Curcumin (-0.82) have negative scores, suggesting they may face challenges in drug development due to poor bioavailability or other unfavorable properties. The table also includes well-known compounds like Alpha-Carotene (0.37), Berberastine (0.34), and Daidzein (0.29), which show moderate drug-likeness, indicating they might require further optimization for therapeutic use.

Based on the docking score, Pa value, pIC50 value, and drug-likeness score, the top five phytochemicals, namely EGCG, diosmin, naringenin, neohesperidin, and rhamnetin, were taken into consideration for further analysis.

### *3.5. Physiochemical properties of the top compounds*

Physiochemical properties of the selected phytocompounds were evaluated using ADMET 3.0 (**Table 2**) (**Figure 5**). Among the five phytocompounds analyzed—Diosmin, EGCG, Naringenin, Neohisperidine, and Rhamnetin— EGCG and Rhamnetin emerge as the most promising candidates for drug development based on their balanced physicochemical properties. EPG exhibits optimal lipophilicity with a logP of 1.372 and logD7.4 of 1.4, suggesting good membrane permeability without excessive hydrophobicity. At the same time, its moderate topological polar surface area (TPSA) of 197.37 indicates reasonable solubility and absorption potential. Additionally, its low flexibility (0.167) enhances binding stability in molecular docking simulations, and its high melting point (317.4°C) suggests thermal stability, though the formulation may require careful consideration. Rhamnetin also demonstrates favorable drug-like properties, including a logP of 1.984, which supports bioavailability, and a moderate TPSA of 120.36, ensuring better membrane permeability than bulkier compounds like Diosmin and Neohisperidine. Its structural rigidity, evidenced by only two rotatable bonds and low flexibility (0.111), further improves metabolic stability and docking predictability. Naringenin presents a mixed profile while smaller in molecular weight (272.07) and thus more compliant with Lipinski's Rule of Five. Its high logP (2.596) favors passive diffusion, and its low TPSA (86.99) makes it ideal for oral absorption. In contrast, Diosmin and Neohisperidine, despite their potential for strong target interactions due to high hydrogen bond donors and acceptors, face significant challenges. Their high molecular weights (>600) and excessive polar groups likely violate drug-likeness guidelines, restricting oral bioavailability. Neohisperidine's negative logP (-0.475) further complicates permeability, suggesting these compounds may be better suited for non-oral applications, such as topical or injectable formulations.

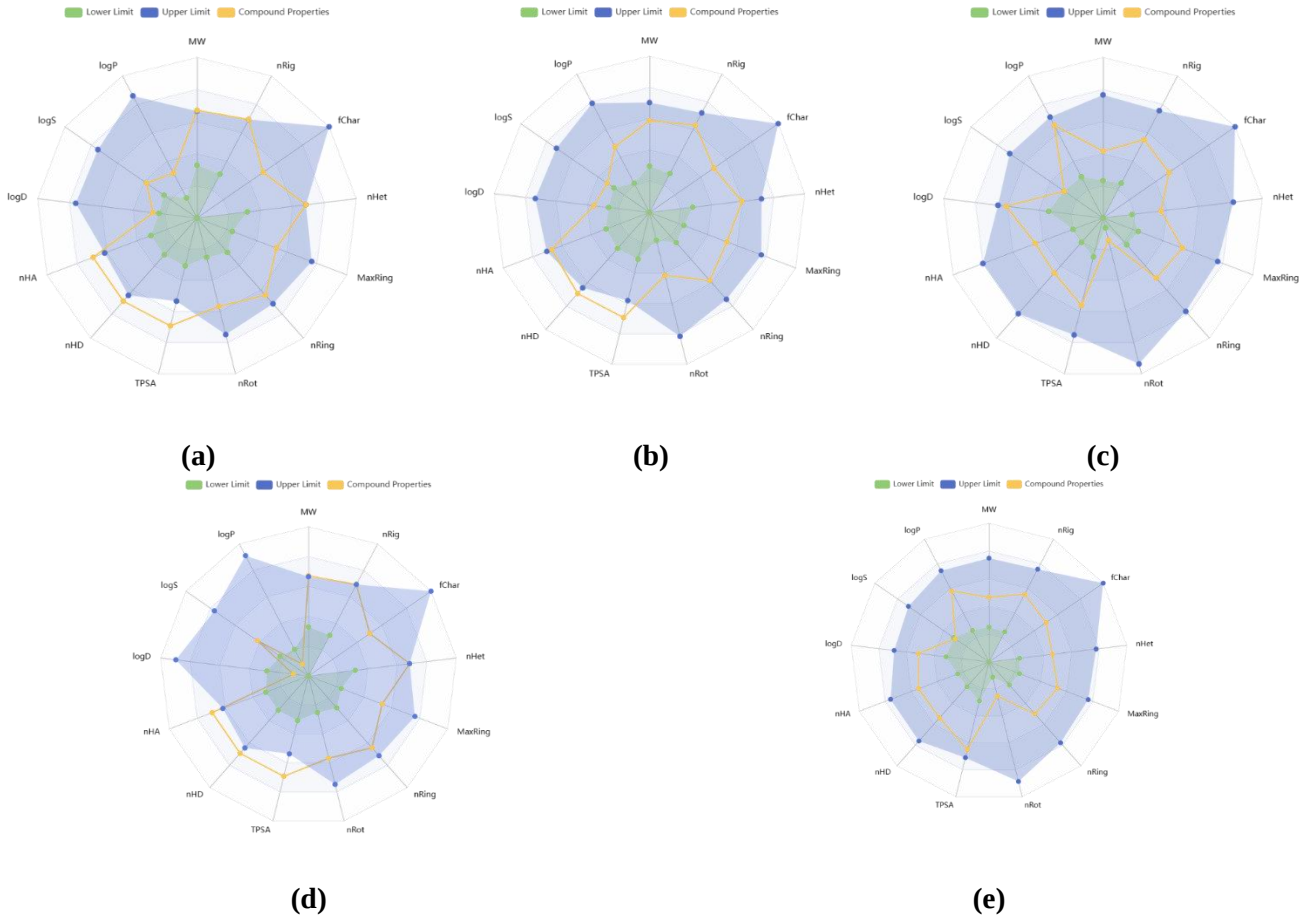


**Figure 5.** Radar chart for the depiction of physiochemical properties of (a) diosmin, (b) (-)-Epigallocatechin-gallate (EPG), (c) naringenin, (d) neohesperidine, and (e) rhamentin.

**Table 2.** Physiochemical properties of the phytochemicals evaluated via ADMET 3.0 server.

| Properties | Diosmin | EPG | Naringenin | Neohesperidine | Rhamnetin |
|---|---|---|---|---|---|
| Molecular Weight | 608.17 | 458.08 | 272.07 | 610.19 | 316.06 |
| Volume | 560.823 | 425.17 | 267.823 | 563.46 | 300.063 |
| Density | 1.084 | 1.077 | 1.016 | 1.083 | 1.053 |
| nHA | 15 | 11 | 5 | 15 | 7 |
| nHD | 8 | 8 | 3 | 8 | 4 |
| nRot | 7 | 4 | 1 | 7 | 2 |
| nRing | 5 | 4 | 3 | 5 | 3 |
| MaxRing | 10 | 10 | 10 | 10 | 10 |
| nHet | 15 | 11 | 5 | 15 | 7 |
| fChar | 0 | 0 | 0 | 0 | 0 |
| nRig | 30 | 24 | 18 | 30 | 18 |
| Flexibility | 0.233 | 0.167 | 0.056 | 0.233 | 0.111 |
| Stereo Centers | 10 | 2 | 1 | 11 | 0 |
| TPSA | 238.2 | 197.37 | 86.99 | 234.29 | 120.36 |
| logS | -2.813 | -3.483 | -4.021 | -2.438 | -4.191 |
| logP | 0.732 | 1.372 | 2.596 | -0.475 | 1.984 |
| logD7.4 | 1.143 | 1.4 | 2.678 | 0.416 | 2.063 |
| pka (Acid) | 5.152 | 6.961 | 8.973 | 6.119 | 6.701 |
| pka (Base) | 4.804 | 2.754 | 5.139 | 4.325 | 2.88 |
| Melting point | 202.608 | 317.394 | 257.278 | 224.755 | 276.147 |
| Boiling point | 334.97 | 453.046 | 381.178 | 382.564 | 344.448 |

### *3.6. Lipinski's rule of 5 analysis*

The top 5 phytocompounds were further assessed for drug candidates using Lipinski's rule of 5 (**Figure 6**). Lipinski's Rule of Five is a widely used guideline to assess the drug-likeness of a molecule, focusing on properties such as molecular mass, hydrogen bond donors and acceptors, lipophilicity (LogP), and molar refractivity. According to these rules, an ideal drug candidate should have a molecular mass under 500 Dalton, fewer than five hydrogen bond donors, fewer than 10 hydrogen bond acceptors, a LogP value below 5, and a molar refractivity between 40 and 130. Diosmin and Neohesperidin both exceed the molecular mass limit, weighing 608 and 610 Dalton, respectively, and they also surpass the recommended thresholds for hydrogen bond donors (8) and acceptors (15). EPG, with a molecular mass of 458 Dalton, is just under the 500 Dalton limit but still fails due to its high number of hydrogen bond donors (8) and acceptors (11). In contrast, Naringenin and Rhamentin comply with most criteria: their molecular masses (272 and 316 Dalton) are well within the limit, and they have acceptable numbers of hydrogen bond donors (3 and 4) and acceptors (5 and 7). Their LogP values (2.509899 and 2.313899) indicate moderate lipophilicity, and their molar refractivity values fall within the recommended range.

### *3.7. ADME/T profiling of the phytocompounds*

ADME/T profiling aids in evaluating the preclinical efficacy of the compounds. **Table 3** shows the ADME/T profile of the selected compounds, while **figure 7** schematically represents the toxicity profile of the phytochemicals. Regarding absorption, oral bioavailability is a critical parameter, with compounds typically requiring at least 30% bioavailability to be considered effective. Naringenin and Rhamnetin meet this criterion, being classified as bioavailable, while Diosmin, EPG, and Neohisperidine fall short, indicating limited systemic exposure upon oral administration. Intestinal absorption, another key factor, generally favors compounds with absorption rates exceeding 70%. Again, Naringenin and Rhamnetin are predicted to be well-absorbed, whereas the others are not, suggesting potential challenges in achieving therapeutic concentrations. The role of P-glycoprotein further differentiates these compounds; Diosmin and Neohisperidine are substrates, meaning they may be actively pumped out of cells, reducing their bioavailability, while the remaining compounds avoid this issue.

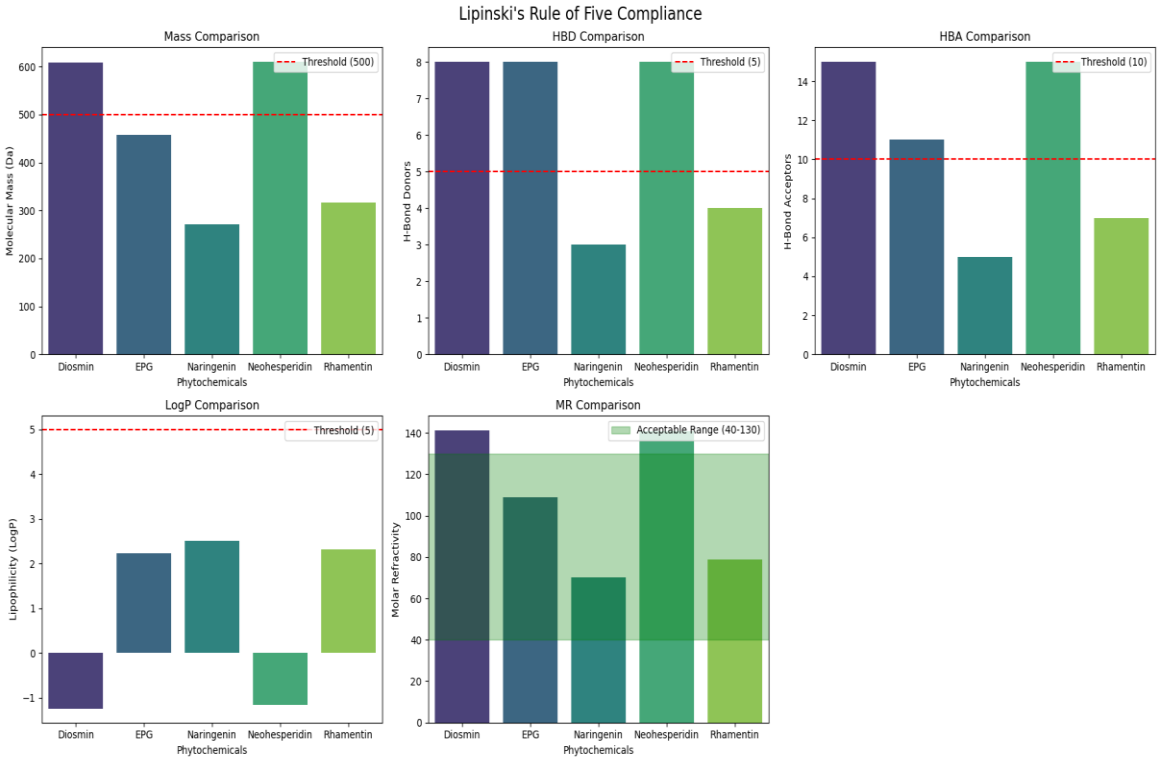


**Figure 6.** Lipinski's rule of five parameters and their predicted values for the selected phytochemicals.

**Table 3.** ADME/T profile of the phytochemicals evaluated via DEEP-PK server.

| Properties | Parameters | Diosmin | EPG | Naringenin | Neohisperidine | Rhamnetin |
|---|---|---|---|---|---|---|
| Absorption | Human Oral Bioavailability | Non-Bioavailable | Non-Bioavailable | Bioavailable | Non-Bioavailable | Bioavailable |
| | Human Intestinal Absorption | Non-Absorbed | Non-Absorbed | Absorbed | Non-Absorbed | Absorbed |
| | Human Oral Bioavailability | Non-Bioavailable | Non-Bioavailable | Bioavailable | Non-Bioavailable | Bioavailable |
| | P-Glycoprotein Inhibitor | Non-Inhibitor | Non-Inhibitor | Non-Inhibitor | Non-Inhibitor | Non-Inhibitor |
| | P-Glycoprotein Substrate Predictions | Substrate | Non-Substrate | Non-Substrate | Substrate | Non-Substrate |
| Distribution | Blood-Brain Barrier Predictions | Non-Penetrable | Non-Penetrable | Non-Penetrable | Non-Penetrable | Non-Penetrable |
| | Fraction Unbound (Human) Predictions | 0.89 | 0.76 | 0.91 | 0.79 | 1.21 |
| | Plasma Protein Binding Predictions | 75.25 | 84.91 | 80.76 | 70.66 | 84.11 |
| Metabolism | CYP 1A2 Inhibitor Predictions | Non-Inhibitor | Non-Inhibitor | Inhibitor | Non-Inhibitor | Inhibitor |
| | CYP 1A2_substrate Predictions | Non-Substrate | Non-Substrate | Substrate | Non-Substrate | Non-Substrate |
| | CYP 2C19 Inhibitor Predictions | Non-Inhibitor | Non-Inhibitor | Inhibitor | Non-Inhibitor | Inhibitor |
| | CYP 2C19_substrate Predictions | Non-Substrate | Non-Substrate | Substrate | Non-Substrate | Non-Substrate |
| | CYP 2C9 Inhibitor Predictions | Non-Inhibitor | Inhibitor | Non-Inhibitor | Non-Inhibitor | Inhibitor |
| | CYP 2C9 Substrate Predictions | Non-Substrate | Non-Substrate | Substrate | Non-Substrate | Substrate |
| | CYP 2D6 Inhibitor Predictions | Non-Inhibitor | Non-Inhibitor | Non-Inhibitor | Non-Inhibitor | Non-Inhibitor |
| | CYP 2D6 Substrate Predictions | Non-Substrate | Non-Substrate | Non-Substrate | Non-Substrate | Non-Substrate |
| | CYP 3A4 Inhibitor Predictions | Non-Inhibitor | Non-Inhibitor | Inhibitor | Non-Inhibitor | Non-Inhibitor |
| | CYP 3A4 Substrate Predictions | Non-Substrate | Non-Substrate | Non-Substrate | Non-Substrate | Non-Substrate |
| | OATP1B1 Predictions | Non-Inhibitor | Inhibitor | Non-Inhibitor | Non-Inhibitor | Non-Inhibitor |
| | OATP1B3 Predictions | Non-Inhibitor | Non-Inhibitor | Non-Inhibitor | Non-Inhibitor | Non-Inhibitor |
| Excretion | Clearance Predictions | 9.67 | 13.72 | 8.89 | 8.72 | 8.58 |
| | Organic Cation Transporter 2 Predictions | Non-Inhibitor | Inhibitor | Non-Inhibitor | Non-Inhibitor | Inhibitor |
| | Half-Life of Drug Predictions | Half-Life < 3hs | Half-Life < 3hs | Half-Life < 3hs | Half-Life >= 3hs | Half-Life < 3hs |
| Toxicity | AMES Mutagenesis Predictions | Safe | Safe | Safe | Safe | Safe |
| | Avian Predictions | Safe | Safe | Safe | Safe | Safe |
| | Biodegradation Predictions | Toxic | Safe | Safe | Toxic | Safe |
| | Carcinogenesis Predictions | Safe | Safe | Safe | Safe | Safe |
| | Eye Corrosion Predictions | Safe | Safe | Safe | Safe | Safe |
| | Maximum Tolerated Dose Predictions | 0.82 | 0.83 | 1.08 | 0.58 | 1.16 |
| | hERG Blockers Predictions | Safe | Safe | Safe | Safe | Safe |
| | NR-AR Predictions | Safe | Safe | Safe | Safe | Safe |
| | NR-AR-LBD Predictions | Safe | Safe | Safe | Safe | Safe |
| | NR-Aromatase Predictions | Safe | Safe | Safe | Safe | Safe |
| | NR-ER Predictions | Safe | Safe | Toxic | Safe | Safe |
| | NR-ER-LBD Predictions | Safe | Safe | Toxic | Safe | Safe |
| | NR-GR Predictions | Safe | Safe | Safe | Safe | Safe |
| | NR-PPAR-gamma Predictions | Safe | Safe | Safe | Safe | Safe |
| | NR-TR Predictions | Safe | Safe | Toxic | Safe | Safe |
| | Respiratory Disease Predictions | Safe | Toxic | Safe | Safe | Safe |
| | SR-ATAD5 Predictions | Safe | Safe | Safe | Safe | Safe |
| | SR-HSE Predictions | Safe | Safe | Safe | Safe | Safe |
| | SR-p53 Predictions | Safe | Safe | Safe | Safe | Safe |

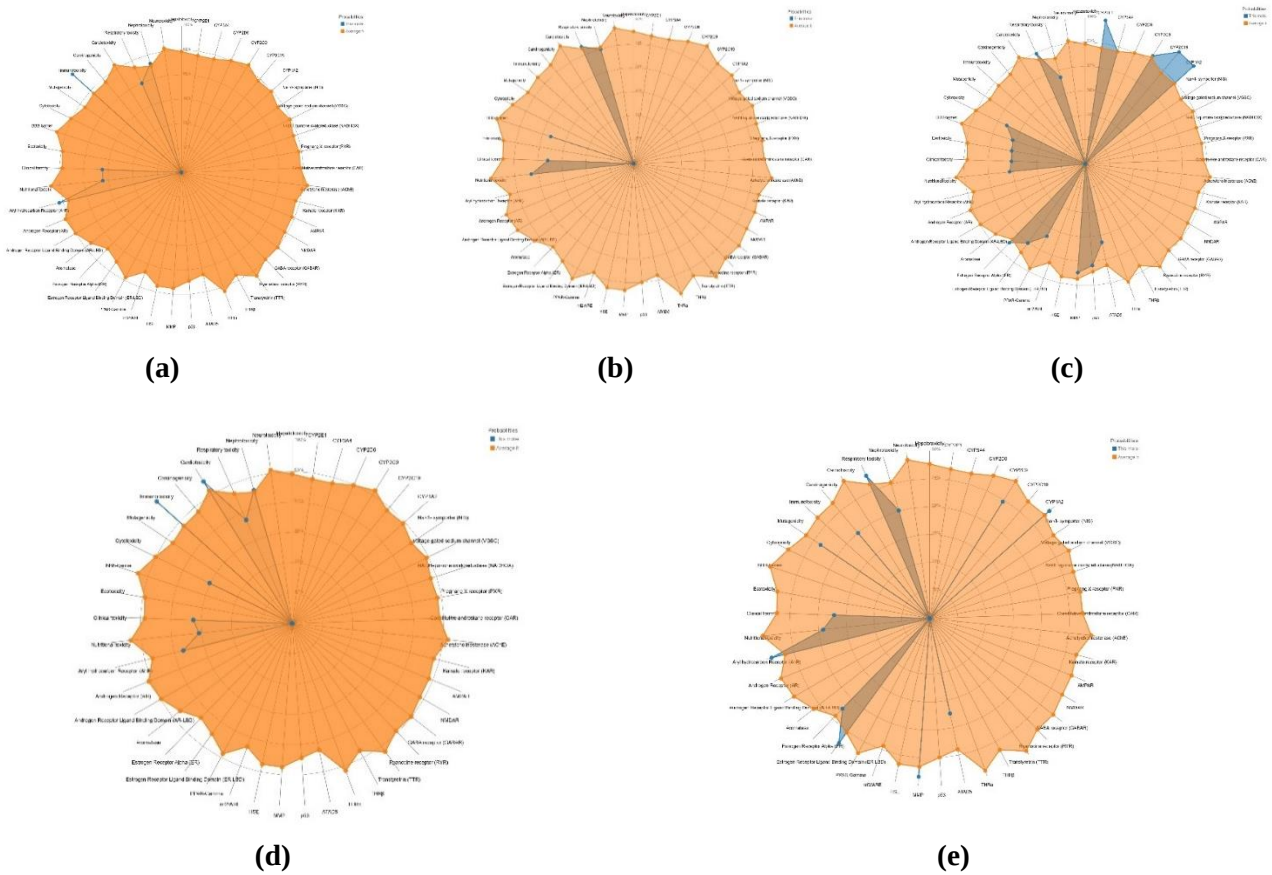


**Figure 7.** Toxicity profile of the phytochemicals as predicted via PROTOX 3.0 server: (a) diosmin, (b) (-)-Epigallocatechin-gallate (EPG), (c) naringenin, (d) neohesperidine, and (e) rhamentin.

Distribution properties reveal additional insights. None of the compounds are predicted to cross the blood-brain barrier, which may be advantageous for avoiding central nervous system side effects but limits their utility in treating neurological conditions. The fraction unbound in plasma, an indicator of the pharmacologically active free drug concentration, falls within the typical desired range of 0.1–1.0 for all compounds except Rhamnetin, which slightly exceeds this at 1.21, suggesting higher free drug levels. Plasma protein binding, which can restrict drug availability, is notably high for EPG (84.91%) and Rhamnetin (84.11%), approaching the 90% threshold where significant binding may limit therapeutic efficacy. Metabolic stability and potential for drug-drug interactions are assessed through cytochrome P450 (CYP) enzyme interactions. Naringenin and Rhamnetin exhibit inhibitory effects on multiple CYP enzymes (1A2, 2C19, and 2C9), raising concerns about their use in combination therapies where they might alter the metabolism of co-administered drugs. In contrast, Diosmin and Neohisperidine show minimal CYP-related activity, making them safer candidates for polypharmacy. While not a broad CYP inhibitor, EPG inhibits CYP 2C9 and OATP1B1, which could still pose interaction risks. Substrate status for these enzymes further complicates the picture; Naringenin, for instance, is a substrate for several CYPs, indicating it may undergo rapid metabolism and clearance. Excretion profiles provide clues about how long these compounds remain active in the body. Clearance rates for all five phytochemicals fall within the moderate range of 5–15 mL/min/kg, with EPG exhibiting the highest clearance (13.72), suggesting faster elimination. Half-life predictions are particularly relevant for dosing frequency; Neohisperidine stands out with a half-life of ≥3 hours, potentially allowing for less frequent dosing than the others, which all have half-lives under 3 hours. The inhibition of the Organic Cation Transporter 2 by EPG and Rhamnetin could additionally influence the excretion of other drugs that rely on this pathway, warranting caution in clinical use. Toxicity assessments are largely favorable, with all compounds deemed safe in

standard mutagenicity and carcinogenicity tests. However, biodegradation toxicity flags Diosmin and Neohisperidine as potential environmental concerns, while EPG is associated with respiratory toxicity, limiting its appeal for certain applications. Naringenin's activity in nuclear receptor pathways (NR-ER, NR-ER-LBD, and NR-TR) suggests possible endocrine-disrupting effects, a significant consideration for long-term use. The maximum tolerated dose (MTD) values, which reflect safety margins, range from 0.58 for Neohisperidine to 1.16 for Rhamnetin, with higher values indicating a more favorable safety profile.

This comparative analysis highlights distinct ADMET profiles among the five phytochemicals. Naringenin and Rhamnetin exhibit favorable absorption but carry risks related to metabolic interactions and endocrine disruption, as in the case of Naringenin. Diosmin and Neohisperidine, while safer in terms of CYP interactions, face challenges with bioavailability and environmental toxicity. EPG occupies a middle ground but shows potential for respiratory toxicity and transporter-mediated interactions. These insights are invaluable for guiding further research, particularly in selecting candidates for specific therapeutic applications while mitigating risks associated with their pharmacokinetic and toxicological properties.

### *3.8. Molecular dynamic simulation*

MD simulation was performed to analyze the binding stability of the receptor-ligand complex. **Figure 8** shows the Rg trajectories for the receptor-ligands complexes. The trajectories suggest that all five phytochemicals exhibit relatively stable Rg values throughout the simulation, with minor fluctuations. This stability implies that the molecules maintain structural integrity without significant unfolding or drastic conformational changes. The small variations in Rg could reflect subtle adjustments in their molecular conformations as they interact with the solvent or undergo thermal fluctuations. Among the compounds, the diosmin and epigallocatechin gallate complex with MMP-9 appear to have slightly higher Rg values, indicating a less compact structure than the others. In contrast, naringenin, neospheridin, and rhamnetin complexes show lower Rg values, suggesting a more tightly packed conformation. Overall, the Rg trajectories indicate that these phytochemicals are structurally stable under simulated conditions, which is a desirable property for potential therapeutic applications where molecular stability is crucial.

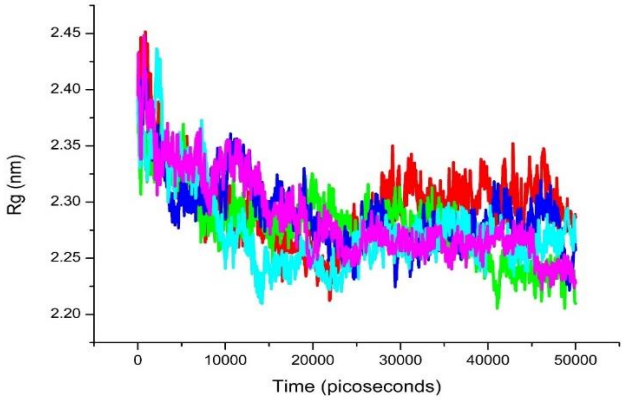


**Figure 8.** The radius of gyration trajectory of phytochemicals in complex with the MMP-9: diosmin (red), (-)-Epigallocatechin-gallate (green), naringenin (blue), neohesperidine (cyan), and rhamnetin (magenta).

The stability of the complexes was further validated by RMSD (**Figure 9**). RMSD is a measure of the conformational stability of a molecule during the simulation, indicating how much the structure deviates from its initial reference frame over time. Initially, all compounds exhibit an expected rise in RMSD values during the equilibration phase as they adjust to the simulation environment. Over time, their trajectories diverge, reflecting differences in structural stability. Diosmin and EGCG display the highest RMSD values (likely exceeding 0.5 nm), indicating significant flexibility, which can be attributed to Diosmin's glycoside moiety and EGCG's bulky gallate group that introduce dynamic conformational changes. Neospheridin shows intermediate stability with RMSD values around 0.3–0.5 nm, suggesting its spirocyclic structure allows for moderate fluctuations while maintaining overall integrity.

In contrast, Naringenin demonstrates exceptional rigidity with the lowest and most stable RMSD profile (consistently below 0.4 nm) due to its simple flavonoid backbone and lack of large substituents that might induce flexibility. Rhamnetin also exhibits stability, with RMSD values ranging between 0.2–0.4 nm, where its methoxy and hydroxyl groups contribute to minor fluctuations before the trajectory plateaus, indicating

efficient equilibration. These findings highlight how structural features govern molecular dynamics. While flexible compounds like Diosmin and EGCG may adapt to diverse binding environments, rigid molecules such as Naringenin and Rhamnetin offer more predictable behavior, making them particularly suitable for drug design where structural consistency is crucial. Based on their dynamic properties, the results provide valuable insights for selecting phytochemicals for further computational or experimental studies.

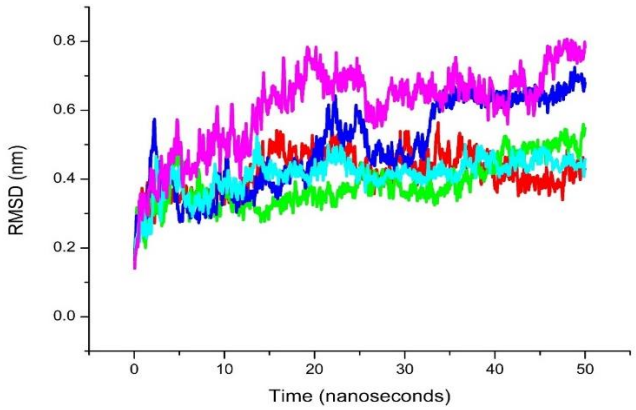


**Figure 9.** Root mean square deviation trajectory of phytochemicals in complex with the MMP-9: diosmin (red), (-)-Epigallocatechin-gallate (green), naringenin (blue), neohesperidine (cyan), and rhamnetin (magenta).

The RMSF trajectory was used to analyze the fluctuation or conformational region of the target protein (**Figure 10**). Higher RMSF values correspond to more flexible regions like loops or unstructured domains. In contrast, lower values suggest stable, rigid regions like secondary structural elements (e.g., alpha-helices or beta-sheets). The plot reveals distinct fluctuation patterns for each phytochemical, providing insights into their binding stability and influence on protein dynamics. For instance, Diosmin and Epigallocatechin gallate likely exhibit lower RMSF peaks in certain regions, indicating stronger binding interactions restricting residue mobility.

In contrast, Neospheridin may show higher fluctuations in specific areas, suggesting weaker binding or localized flexibility. Naringenin and Rhamnetin might display intermediate RMSF values, reflecting a balance between stability and adaptability. These findings are crucial for understanding how each phytochemical modulates protein behavior. This can guide further drug design and optimization by identifying compounds that enhance structural stability or target specific dynamic regions.

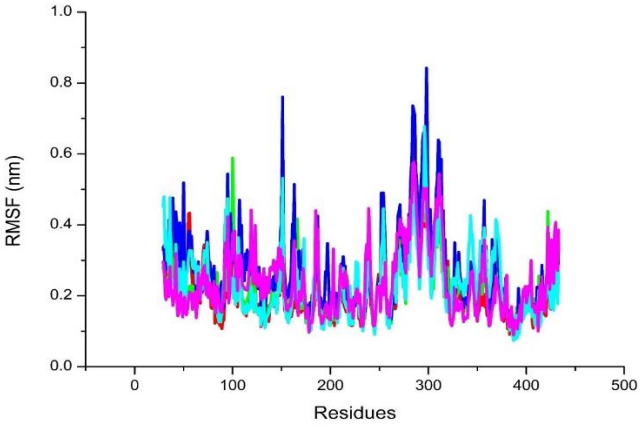


**Figure 10.** Root mean square fluctuation trajectory of phytochemicals in complex with the MMP-9: diosmin (red), (-)-Epigallocatechin-gallate (green), naringenin (blue), neohesperidine (cyan), and rhamnetin (magenta).

The SASA trajectory was used to analyze the structural compactness of the complexes (**Figure 11**). Among these, Naringenin exhibits the most favorable SASA profile, with the lowest and most stable range (approximately 5,000–15,000 nm²), indicating a compact and rigid structure that minimizes solvent exposure. This stability suggests strong structural integrity, which could enhance its bioavailability and target-binding efficiency. In contrast, Neospheridin displays the largest and most variable SASA range (10,000–50,000 nm²), reflecting significant conformational flexibility and dynamic solvent interactions. While this may facilitate binding adaptability, the high fluctuations could imply less stability in the solution. Epigallocatechin gallate (EGCG) and Rhamnetin show intermediate SASA ranges (EGCG: ~10,000–30,000 nm²; Rhamnetin: ~10,000–25,000 nm²), with moderate fluctuations, suggesting a balance between flexibility and stability. EGCG's dynamic behavior aligns with its multifunctional antioxidant role, whereas Rhamnetin's mid-range stability supports its potential as a bioactive compound. Diosmin maintains a relatively stable but slightly higher SASA range (~15,000–25,000 nm²) than Naringenin, indicating consistent solvent exposure with minor adjustments. While not as compact as Naringenin, its steady profile may contribute to its pharmacological efficacy.

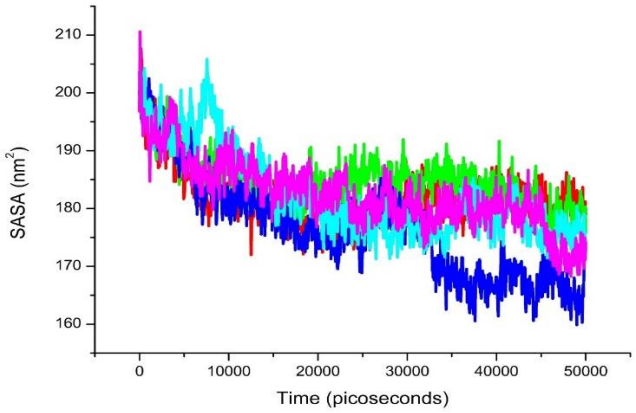


**Figure 11.** Solvent accessible surface area trajectory of phytochemicals in complex with the MMP-9: diosmin (red), (-)-Epigallocatechin-gallate (green), naringenin (blue), neohesperidine (cyan), and rhamnetin (magenta).

Hydrogen bond trajectories provide insights into these ligands' binding affinity and interaction stability with the MMP9 protein, which is crucial for understanding their potential as therapeutic agents or inhibitors (**Figure 12**).

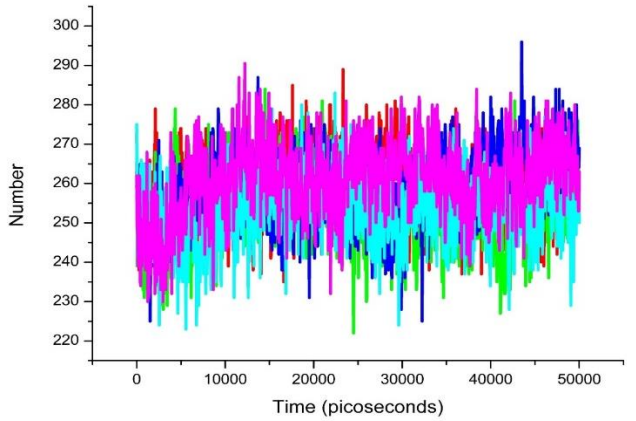


**Figure 12.** Hydrogen bond number trajectory of phytochemicals in complex with the MMP-9: diosmin (red), (-)-Epigallocatechin-gallate (green), naringenin (blue), neohesperidine (cyan), and rhamnetin (magenta).

The hydrogen bonding trajectories reveal distinct interaction profiles for each ligand with MMP-9: Diosmin exhibits stable hydrogen bonds, suggesting strong binding and therapeutic potential for inflammation or cancer, while Epigallocatechin gallate (EGCG) displays persistent, high-affinity interactions due to its polyphenolic structure, making it a promising MMP9 inhibitor. Naringenin shows variable bonding, indicating weaker but dynamic binding that could be optimized, whereas Neospheridin forms selective, moderately stable interactions suitable for balanced inhibition. Rhamnetin demonstrates intermediate bonding with occasional fluctuations, leveraging its methoxy-flavonoid structure for versatile modulation. These findings highlight EGCG and Diosmin as top candidates for drug development, given their robust and consistent hydrogen bonding with MMP9, while the others offer tunable alternatives for specific therapeutic needs.

### *3.9. Interaction between phytochemicals and active site of target protein*

**Table 4** details the interactions between various phytochemicals and the active site of the MMP9 protein, highlighting the types of interactions, the residues involved, and the bond lengths where applicable. Diosmin exhibits van der Waals (VDW) interactions with residues Tyr48, Arg51, Tyr52, Pro97, Arg98, Gly183, Asp185, and Leu187. It also forms hydrogen bonds with Met94 (3.03 Å), Thr96 (2.22 Å), Lys184 (2.92 Å), and Gly186 (2.61 Å), as well as alkyl interactions with Leu39 (3.78 Å) and Leu44 (3.98 Å). Epigallocatechin-gallate engages in VDW interactions with Leu132, Val216, Val217, Val218, Tyr277, and Arg279. Its hydrogen bonds involve Glu130 (2.49 Å), Asp131 (2.25 Å), Thr220 (2.69 Å), Arg221 (3.06 Å), and Thr331 (2.49 Å). Additionally, it forms alkyl interactions with Pro133 (5.10 Å), Pro219 (4.72 Å), Arg221 (5.50 Å), Pro272 (5.16 Å and 5.42 Å), and Ala333 (4.99 Å). Naringenin shows VDW interactions with Asn38, Leu44, Glu47, Tyr48, Met94, Thr96, Pro97, Arg98, Asp185, Gly186, and Leu187, along with a hydrogen bond to Tyr52 (1.80 Å). Neohesperidin participates in VDW interactions with Arg36, Thr37, Leu44, Tyr48, Arg51, Met94, Arg95, Pro97, Arg98, Lys184, Asp185, Gly186, and Leu187. It forms hydrogen bonds with Leu35 (2.63 Å), Asn38 (2.40 Å and 2.58 Å), Glu47 (2.06 Å), Tyr52 (3.06 Å), and Thr96 (2.69 Å), as well as alkyl and pi-sigma interactions with Leu35 (4.99 Å) and Leu39 (4.60 Å), respectively. Rhamnetin displays VDW interactions with Arg98, Cys99, Val398, Leu418, Tyr420, Met422, Tyr423, and Pro430. It forms hydrogen bonds with Glu416 (2.52 Å), Pro421 (2.32 Å), Arg424 (2.82 Å), and Thr426 (2.83 Å), along with alkyl interactions involving Leu397 (5.29 Å), Pro415 (5.49 Å), and Arg424 (5.05 Å). It also exhibits pi-stacked and pi-sigma interactions with His401 (5.12 Å) and Thr426 (3.55 Å). **Figure 13** schematically represents the interaction between the selected phytochemicals and the target protein's active site.

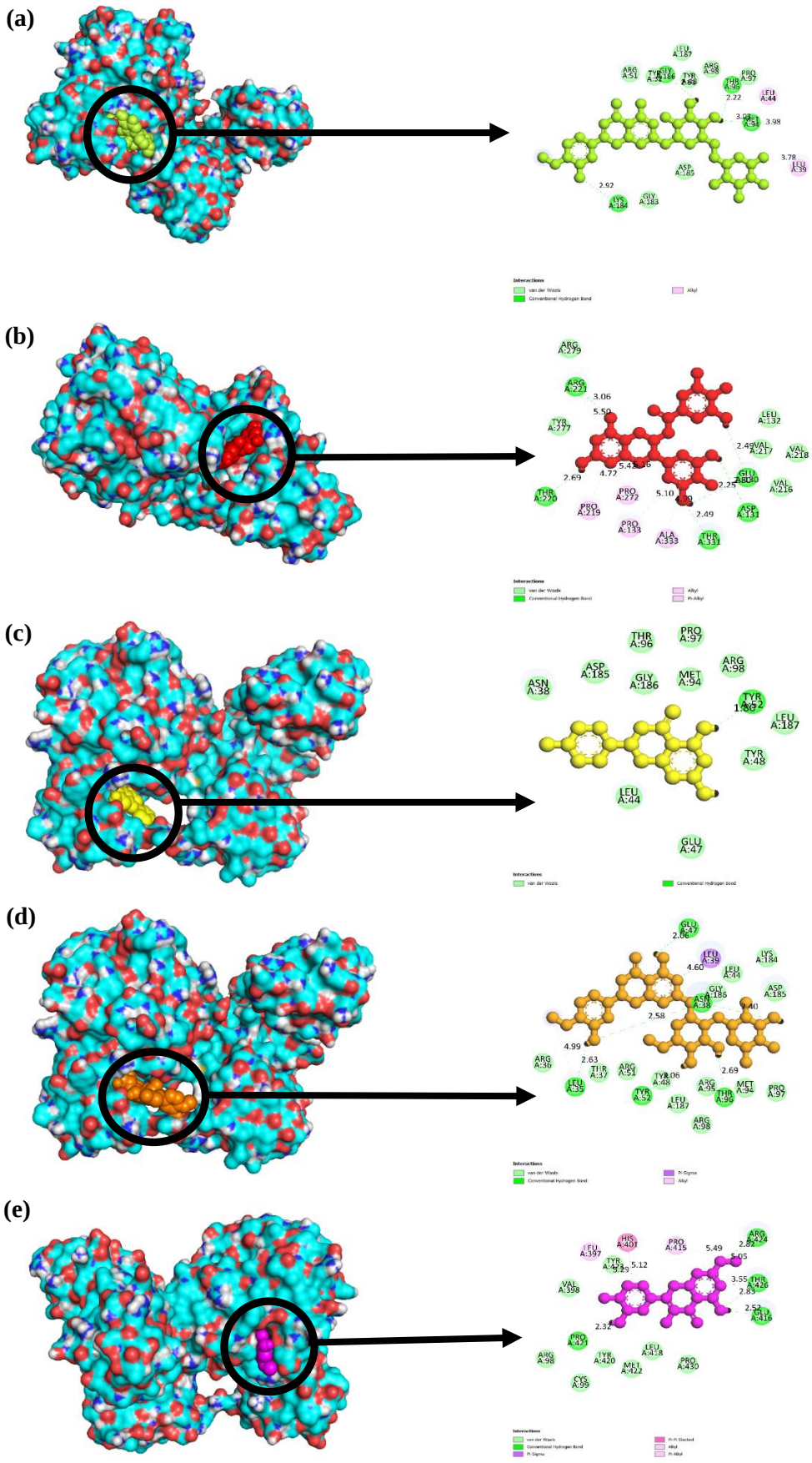


**Figure 13.** Schematic representation of the interaction between phytochemicals and the active site of the MMP-9 protein: (a) diosmin, (b) (-)-Epigallocatechin-gallate (EPG), (c) naringenin, (d) neohesperidine, and (e) rhamnetin.

**Table 4.** The phytochemicals (ligands) interact with the active site of the target protein MMP-9, demonstrating various types of interactions such as van der Waals, alkyl, and hydrogen bonding interactions. The table details the interacting residues and the type of interaction observed.

| Name | Type of interaction | Interacting residues | Bond length |
|---|---|---|---|
| Diosmin | Van der Waals | Tyr48, Arg51, Tyr52, Pro97, Arg98, Gly183, Asp185, Leu187 | --- |
| | Hydrogen bond | Met94 | 3.03 |
| | | Thr96 | 2.22 |
| | | Lys184 | 2.92 |
| | | Gly186 | 2.61 |
| | Alkyl | Leu39 | 3.78 |
| | | Leu44 | 3.98 |
| Epigallocatechin-gallate | Van der Waals | Leu132, Val216, Val217, Val218, Tyr277, Arg279 | --- |
| | Hydrogen bond | Glu130 | 2.49 |
| | | Asp131 | 2.25 |
| | | Thr220 | 2.69 |
| | | Arg221 | 3.06 |
| | | Thr331 | 2.49 |
| | Alkyl | Pro133 | 5.10 |
| | | Pro219 | 4.72 |
| | | Arg221 | 5.50 |
| | | Pro272 | 5.16, 5.42 |
| | | Ala333 | 4.99 |
| Naringenin | Van der Waals | Asn38, Leu44, Glu47, Tyr48, Met94, Thr96, Pro97, Arg98, Asp185, Gly186, Leu187 | --- |
| | Hydrogen bond | Tyr52 | 1.80 |
| Neohesperidin | Van der Waals | Arg36, Thr37, Leu44, Tyr48, Arg51, Met94, Arg95, Pro97, Arg98, Lys184, Asp185, Gly186. Leu187 | --- |
| | Hydrogen bond | Leu35 | 2.63 |
| | | Asn38 | 2.40, 2.58 |
| | | Glu47 | 2.06 |
| | | Tyr52 | 3.06 |
| | | Thr96 | 2.69 |
| | Alkyl | Leu35 | 4.99 |
| | Pi-sigma | Leu39 | 4.60 |
| Rhamnetin | Van der Waals | Arg98, Cys99, Val398, Leu418, Tyr420, Met422, Tyr423, Pro430 | --- |
| | Hydrogen bond | Glu416 | 2.52 |
| | | Pro421 | 2.32 |
| | | Arg424 | 2.82 |
| | | Thr426 | 2.83 |
| | Alkyl | Leu397 | 5.29 |
| | | Pro415 | 5.49 |
| | | Arg424 | 5.05 |
| | Pi-stacked | His401 | 5.12 |
| | Pi-sigma | Thr426 | 3.55 |

The generated data demonstrates the significant potential of phytochemicals, particularly naringenin, and rhamnetin, as natural inhibitors of MMP-9, a key enzyme implicated in cancer progression, metastasis, and angiogenesis. These compounds exhibited strong binding affinities through molecular docking to MMP-9's catalytic domain, supported by favorable PASS prediction scores (Pa>0.75). Their excellent ADME/T

profiles, including high bioavailability, metabolic stability, and low toxicity, further accentuate their suitability for preclinical drug development. Molecular dynamics simulations confirmed the stability of MMP-9 complexes with naringenin and rhamnetin, showing minimal structural fluctuations and persistent hydrogen bonding interactions, key indicators of effective inhibition. Compared to other screened phytochemicals, these two compounds stand out due to their optimal balance of potency and drug-like properties, making them promising candidates for further experimental validation. Previous studies have explored flavonoids as matrix metalloproteinase-9 (MMP9) inhibitors. For instance, a study utilized molecular docking to evaluate flavonoids like quercetin for their binding affinity to MMP9, reporting strong interactions through hydrogen bonding with catalytic residues such as His401, which aligns with our methodology using AutoDock Vina to identify hit compounds [54]. Similarly, we screened flavonoids like kaempferol against MMP9 and MMP2, finding binding energies comparable to known inhibitors supporting the potential of flavonoids like naringenin and rhamnetin identified in our study [55]. A study combined docking with molecular dynamics simulations to confirm luteolin's stable binding to MMP9, a strategy that complements our approach and underscores the role of flavonoids in inhibiting MMP9-mediated ECM degradation [56]. Our study advances these efforts by screening a diverse phytochemical library and identifying novel candidates like neohesperidin while addressing limitations in prior works, such as limited experimental validation, by integrating in silico results with experimental evidence. The anti-cancer activities of our hit compounds, particularly their effects on MMP9 and related pathways, are well-supported by experimental studies. Diosmin, a flavone glycoside, induces oxidative stress, DNA damage, and apoptosis in cancer cells, with in vitro studies on HepG2 cells demonstrating reduced MMP9 expression via NF-κB inhibition and in vivo hepatocellular carcinoma models confirming decreased tumor growth and metastasis [57]. Epigallocatechin Gallate (EGCG) exhibits antiproliferative, antiangiogenic, and pro-apoptotic effects across cancers like breast and lung, with in vitro data from H1299 and MDA-MB-231 cells showing MMP9 inhibition through ERK1/2 and JNK pathway suppression, further enhanced in vivo by nanoemulsions reducing IC50 from 36.03 μM to 4.71 μM in lung cancer xenografts [58, 59]. Naringenin, a flavanone, inhibits proliferation and metastasis in breast and prostate cancers, with in vitro MCF7 cell studies showing reduced MMP9 expression and in vivo models confirming prolonged survival through PI3K/AKT modulation [60]. Rhamnetin, a methylated flavonol, induces apoptosis and cell cycle arrest, with in vitro MCF7 cell studies and in vivo breast cancer xenografts confirming MMP9 inhibition via VEGF and NF-κB downregulation [61]. Comparing our in silico results with experimental data reveals both consistencies and discrepancies. Our docking studies predicted strong binding affinities for all five compounds to MMP9, likely due to hydrogen bonds and hydrophobic interactions with the active site, such as the S1' pocket. For EGCG, diosmin, and naringenin, in vitro and in vivo studies strongly support these predictions, with potent MMP9 inhibition observed in cancer cell lines and xenograft models. However, effective concentrations are often higher than predicted, suggesting pharmacokinetic limitations not captured by in silico models. Neohesperidin's limited experimental data indicate weaker MMP9 inhibition than predicted, possibly due to poor cellular uptake. At the same time, rhamnetin's in vivo effects are less pronounced than EGCG's, highlighting the potential overestimation of its potency [62]. These findings underscore the strengths of in silico screening in efficiently identifying promising candidates and its limitations in accounting for bioavailability and dynamic protein-ligand interactions. To address this, we propose combining docking with molecular dynamics simulations, as reported in previous studies, and conducting targeted in vitro assays in cancer cell lines like MCF7 and H1299 to validate neohesperidin's activity, alongside in vivo studies to confirm rhamnetin's efficacy. These phytochemicals hold promise as adjuvants in cancer therapy due to their low toxicity and MMP9-targeting potential, which warrant further validation through clinical trials to translate these findings into therapeutic applications.

## 4. Conclusion

This Study highlights the potential of selected phytochemicals, particularly naringenin and rhamnetin,

as natural inhibitors of MMP-9, an enzyme central to cancer metastasis and angiogenesis. These compounds demonstrated strong binding affinities and stable interactions with MMP-9's catalytic domain through molecular docking and molecular dynamics simulations. Their favorable ADME/T profiles, including high bioavailability and low predicted toxicity, further support their suitability as preclinical drug candidates. The results are consistent with previous findings on flavonoids like quercetin, kaempferol, and luteolin, reinforcing the broader potential of this class in targeting MMP9-mediated pathways in cancer. Comparative analysis with experimental studies affirms the anti-cancer effects of naringenin, rhamnetin, EGCG, and diosmin, although some discrepancies, particularly with neohesperidin, highlight the limitations of purely in silico models. Therefore, integrating computational predictions with targeted in vitro and in vivo validation is essential to bridge the translational gap. Due to their low toxicity and promising inhibitory action on MMP-9, these phytochemicals offer valuable prospects as adjuncts in cancer therapy. Further experimental and clinical investigations are warranted to confirm their therapeutic efficacy and optimize their pharmacokinetic properties for clinical use.

**Acknowledgment**

The authors would like to acknowledge the Indian Biological Sciences and Research Institute, Noida, and the Department of Zoology, A.M.U., for providing the required facilities for the work.

**Conflict of interest**

Authors declare no conflict of interest.

**Data availability**

The datasets used and/or analyzed during the current study are available from the corresponding author on reasonable request.

**Athors Contributions**

**M.A:** Study design, conceptualization, and supervision. **K.A:** Data collection, software, graphics. **F.H.** & **B.S:** Data collection and literature search. **K.R:** Data analysis and writing the original draft. **I.A:** Writing original draft, review, and editing. **V.P:** Review & editing. **G.G.H.A.S:** Supervision & proofreading manuscript.

**Athors Orcid numbers:**

Faiqua Haque: 0009-0000-4376-8501
Bisma Showkat: 0009-0000-4938-8315
Khalid Rasheed: 0000-0003-4891-4373
Imran Ansari: 0009-0008-6077-0425
Varsha Pawar: 0009-0001-9936-0270
Mudassir Alam : 0000-0001-8255-0273
G.G.H.A. Shadab: 0000-0002-9845-3758

**Funding**

Authors declare that no funding was received for this work.

**Using artificial intelligence chatbots**

There was no use of artificial intelligence in the making of this article.

**References**

1. Thun MJ, DeLancey JO, Center MM, Jemal A, Ward EM. The global burden of cancer: priorities for prevention. Carcinogenesis (2010) 31(1):100-10.
2. Hanahan D, Weinberg RA. Hallmarks of cancer: the next generation. Cell (2011) 144(5):646-74.
3. Bhat AS, Ahmed M, Abbas K, Mustafa M, Alam M, Salem MA, et al. Cancer initiation and progression: a comprehensive review of carcinogenic substances, anti-cancer therapies, and regulatory frameworks. Asian J Res Biochem (2024) 14(4):111-25.
4. Seyfried TN, Huysentruyt LC. On the origin of cancer metastasis. Crit Rev Oncog (2013) 18(1-2):43-73.
5. Mustafa M, Abbas K, Alam M, Habib S, Zulfareen, Hasan GM, et al. Investigating underlying molecular mechanisms, signaling pathways, emerging therapeutic approaches in pancreatic cancer. Front Oncol (2024) 14:1427802.
6. Yue B. Biology of the extracellular matrix: an overview. J Glaucoma (2014) 23(8 Suppl 1):S20-3.
7. Dzobo K, Dandara C. The Extracellular Matrix: Its Composition, Function, Remodeling, and Role in Tumorigenesis. Biomimetics (Basel) (2023) 8(2).
8. Bonnans C, Chou J, Werb Z. Remodelling the extracellular matrix in development and disease. Nat Rev Mol Cell Biol (2014) 15(12):786-801.

9. Kessenbrock K, Plaks V, Werb Z. Matrix metalloproteinases: regulators of the tumor microenvironment. Cell (2010) 141(1):52-67.
10. Niland S, Riscanevo AX, Eble JA. Matrix Metalloproteinases Shape the Tumor Microenvironment in Cancer Progression. Int J Mol Sci (2021) 23(1).
11. Laronha H, Caldeira J. Structure and Function of Human Matrix Metalloproteinases. Cells (2020) 9(5).
12. Gonzalez-Avila G, Sommer B, Mendoza-Posada DA, Ramos C, Garcia-Hernandez AA, Falfan-Valencia R. Matrix metalloproteinases participation in the metastatic process and their diagnostic and therapeutic applications in cancer. Crit Rev Oncol Hematol (2019) 137:57-83.
13. Sabeh F, Shimizu-Hirota R, Weiss SJ. Protease-dependent versus -independent cancer cell invasion programs: three-dimensional amoeboid movement revisited. J Cell Biol (2009) 185(1):11-9.
14. Augoff K, Hryniewicz-Jankowska A, Tabola R, Stach K. MMP9: A Tough Target for Targeted Therapy for Cancer. Cancers (Basel) (2022) 14(7).
15. Barillari G. The Impact of Matrix Metalloproteinase-9 on the Sequential Steps of the Metastatic Process. Int J Mol Sci (2020) 21(12).
16. Page-McCaw A, Ewald AJ, Werb Z. Matrix metalloproteinases and the regulation of tissue remodelling. Nat Rev Mol Cell Biol (2007) 8(3):221-33.
17. Deryugina EI, Kiosses WB. Intratumoral Cancer Cell Intravasation Can Occur Independent of Invasion into the Adjacent Stroma. Cell Rep (2017) 19(3):601-16.
18. Deryugina EI, Quigley JP. Tumor angiogenesis: MMP-mediated induction of intravasation- and metastasis-sustaining neovasculature. Matrix Biol (2015) 44-46:94-112.
19. Parham S, Kharazi AZ, Bakhsheshi-Rad HR, Nur H, Ismail AF, Sharif S, et al. Antioxidant, Antimicrobial and Antiviral Properties of Herbal Materials. Antioxidants (Basel) (2020) 9(12).
20. Ansari MS, Abbas K, Alam M, Usmani N, Khan A, Khan AA, et al. Investigating the anxiolytic potential of Withania somnifera: a GC–MS and in silico Study targeting MAO-A inhibition. Discover Plants (2025) 2(1):89.
21. Alam M, Abbas K, Raza MT, Abedi SMH, Haq H, Mustafa M. Identification of Aquaporin 3 Inhibitors from Santalum album Phytochemicals for Melanoma treatment: A Computational Study: Targeting Aquaporin 3: Santalum Album in Melanoma Therapy. Iranian Journal of Pharmaceutical Sciences (2024) 20(4):293- 314.
22. Alonso-Castro AJ, Villarreal ML, Salazar-Olivo LA, Gomez-Sanchez M, Dominguez F, Garcia-Carranca A. Mexican medicinal plants used for cancer treatment: pharmacological, phytochemical and ethnobotanical studies. J Ethnopharmacol (2011) 133(3):945-72.
23. Berdigaliyev N, Aljofan M. An overview of drug discovery and development. Future Med Chem (2020) 12(10):939-47.
24. Alam M, Abbas K, Ahmad A, Showkat N, Sen R. Identification of Hsp90 inhibitors from Ananas comosus potential phytochemicals for lung cancer treatment. The Journal of Phytopharmacology (2024) 13:12-9.
25. Tilaoui M, Ait Mouse H, Zyad A. Update and New Insights on Future Cancer Drug Candidates From Plant-Based Alkaloids. Front Pharmacol (2021) 12:719694.
26. Raina H, Soni G, Jauhari N, Sharma N, Bharadvaja N. Phytochemical importance of medicinal plants as potential sources of anti-cancer agents. Turkish Journal of Botany (2014) 38(6):1027-35.
27. Deep A, Kumar D, Bansal N, Narasimhan B, Marwaha RK, Sharma PC. Understanding mechanistic aspects and therapeutic potential of natural substances as anti-cancer agents. Phytomedicine Plus (2023) 3(2):100418.
28. Akter R, Uddin SJ, Grice ID, Tiralongo E. Cytotoxic activity screening of Bangladeshi medicinal plant extracts. J Nat Med (2014) 68(1):246-52.
29. Solowey E, Lichtenstein M, Sallon S, Paavilainen H, Solowey E, Lorberboum-Galski H. Evaluating medicinal plants for anti-cancer activity. ScientificWorldJournal (2014) 2014:721402.
30. Brassart-Pasco S, Brézillon S, Brassart B, Ramont L, Oudart JB, Monboisse JC. Tumor Microenvironment: Extracellular Matrix Alterations Influence Tumor Progression. Front Oncol (2020) 10:397.
31. Winer A, Adams S, Mignatti P. Matrix Metalloproteinase Inhibitors in Cancer Therapy: Turning Past Failures Into Future Successes. Mol Cancer Ther (2018) 17(6):1147-55.
32. Mir SA, Dar A, Hamid L, Nisar N, Malik JA, Ali T, et al. Flavonoids as promising molecules in the cancer

therapy: An insight. Current Research in Pharmacology and Drug Discovery (2024) 6:100167.
33. Ponte LGS, Pavan ICB, Mancini MCS, da Silva LGS, Morelli AP, Severino MB, et al. The Hallmarks of Flavonoids in Cancer. Molecules (2021) 26(7).
34. Zhang C, Kim SK. Matrix metalloproteinase inhibitors (MMPIs) from marine natural products: the current situation and future prospects. Mar Drugs (2009) 7(2):71-84.
35. Lans C, van Asseldonk T. Dr. Duke's Phytochemical and Ethnobotanical Databases, a Cornerstone in the Validation of Ethnoveterinary Medicinal Plants, as Demonstrated by Data on Pets in British Columbia. In: Máthé Á, editor. Medicinal and Aromatic Plants of North America. Cham: Springer International Publishing; 2020. p. 219-46.
36. Kim S, Thiessen PA, Bolton EE, Chen J, Fu G, Gindulyte A, et al. PubChem Substance and Compound databases. Nucleic Acids Res (2016) 44(D1):D1202-13.
37. Pettersen EF, Goddard TD, Huang CC, Couch GS, Greenblatt DM, Meng EC, et al. UCSF Chimera—a visualization system for exploratory research and analysis. Journal of computational chemistry (2004) 25(13):1605-12.
38. Maier JA, Martinez C, Kasavajhala K, Wickstrom L, Hauser KE, Simmerling C. ff14SB: Improving the Accuracy of Protein Side Chain and Backbone Parameters from ff99SB. J Chem Theory Comput (2015) 11(8):3696-713.
39. Abbas K, Alam M, Ansari MS, Khan A, Raza MT, Khan Z, et al. Isorauhimbine and Vinburnine as Novel 5-HT2A Receptor Antagonists From Rauwolfia serpentina for the Treatment of Insomnia: An In Silico Investigation. (2024).
40. Eberhardt J, Santos-Martins D, Tillack AF, Forli S. AutoDock Vina 1.2.0: New Docking Methods, Expanded Force Field, and Python Bindings. Journal of Chemical Information and Modeling (2021) 61(8):3891-8.
41. Pawar RP, Rohane SH. Role of autodock vina in PyRx molecular docking. (2021).
42. Yoshikawa N, Hutchison GR. Fast, efficient fragment-based coordinate generation for Open Babel. Journal of Cheminformatics (2019) 11(1):49.
43. Druzhilovskiy DS, Rudik AV, Filimonov DA, Gloriozova TA, Lagunin AA, Dmitriev AV, et al. Computational platform Way2Drug: from the prediction of biological activity to drug repurposing. Russian Chemical Bulletin (2017) 66(10):1832-41.
44. Fu L, Shi S, Yi J, Wang N, He Y, Wu Z, et al. ADMETlab 3.0: an updated comprehensive online ADMET prediction platform enhanced with broader coverage, improved performance, API functionality and decision support. Nucleic Acids Research (2024) 52(W1):W422-W31.
45. Lipinski CA. Lead- and drug-like compounds: the rule-of-five revolution. Drug Discovery Today: Technologies (2004) 1(4):337-41.
46. Kufareva I, Lenoir M, Dancea F, Sridhar P, Raush E, Bissig C, et al. Discovery of novel membrane binding structures and functions. Biochem Cell Biol (2014) 92(6):555-63.
47. Yin X, Wang X, Li Y, Wang J, Wang Y, Deng Y, et al. CODD-Pred: A Web Server for Efficient Target Identification and Bioactivity Prediction of Small Molecules. Journal of Chemical Information and Modeling (2023) 63(20):6169-76.
48. Banerjee P, Eckert AO, Schrey AK, Preissner R. ProTox-II: a webserver for the prediction of toxicity of chemicals. Nucleic Acids Res (2018) 46(W1):W257-w63.
49. Yadav P, Azram M, Faraz M, Alam M, Khan S. In Silico Screening of Rauwolfia Serpentina Phytochemicals as Orexin Receptor-2 Agonists for the Management of Narcolepsy.
50. Tumskiy RS, Tumskaia AV. Multistep rational molecular design and combined docking for discovery of novel classes of inhibitors of SARS-CoV-2 main protease 3CLpro. Chem Phys Lett (2021) 780:138894.
51. Ghahremanian S, Rashidi MM, Raeisi K, Toghraie D. Molecular dynamics simulation approach for discovering potential inhibitors against SARS-CoV-2: A structural review. J Mol Liq (2022) 354:118901.
52. Ching KWC, Nazri MNM, Rachman ARA, Mustafa KMF, Mokhtar NF. In silico Study of shape complementarity, binding affinity, and protein–ligand interactions of systematic evolution of ligands by exponential enrichment-aptamer to programmed death ligand-1 using patchdock. Journal of Preventive, Diagnostic and Treatment Strategies in Medicine (2022) 1(2):127-33.
53. Yin X, Wang X, Li Y, Wang J, Wang Y, Deng Y, et al. CODD-Pred: A Web Server for Efficient Target Identification and Bioactivity Prediction of Small Molecules. J Chem Inf Model (2023) 63(20):6169-76.

54. Saragusti AC, Ortega MG, Cabrera JL, Estrin DA, Marti MA, Chiabrando GA. Inhibitory effect of quercetin on matrix metalloproteinase 9 activity Molecular mechanism and structure–activity relationship of the flavonoid–enzyme interaction. *European Journal of Pharmacology* (2010) 644(1):138-45.
55. Yarmohammadi E, Naimiyan A, Taherkhani A. Flavonoids as dual-action agents for anti-cancer and anti-tooth caries: a molecular docking and dynamics simulation on MMP2 inhibition. IJS Oncology (2024) 9(2):25-33.
56. Zhou Z-G, Yao Q-Z, Lei D, Zhang Q-Q, Zhang J. Investigations on the mechanisms of interactions between matrix metalloproteinase 9 and its flavonoid inhibitors using a combination of molecular docking, hybrid quantum mechanical/molecular mechanical calculations, and molecular dynamics simulations. Canadian Journal of Chemistry (2014) 92:821-30.
57. Rahman L, Talha Khalil A, Ahsan Shahid S, Shinwari ZK, Almarhoon ZM, Alalmaie A, et al. Diosmin: A promising phytochemical for functional foods, nutraceuticals and cancer therapy. Food Sci Nutr (2024) 12(9):6070-92.
58. Tanabe H, Suzuki T, Ohishi T, Isemura M, Nakamura Y, Unno K. Effects of Epigallocatechin-3-Gallate on Matrix Metalloproteinases in Terms of Its Anti-cancer Activity. Molecules (2023) 28(2):525.
59. Du GJ, Zhang Z, Wen XD, Yu C, Calway T, Yuan CS, et al. Epigallocatechin Gallate (EGCG) is the most effective cancer chemopreventive polyphenol in green tea. Nutrients (2012) 4(11):1679-91.
60. Hermawan A, Ikawati M, Jenie RI, Khumaira A, Putri H, Nurhayati IP, et al. Identification of potential therapeutic target of naringenin in breast cancer stem cells inhibition by bioinformatics and in vitro studies. Saudi Pharm J (2021) 29(1):12-26.
61. Lan L, Wang Y, Pan Z, Wang B, Yue Z, Jiang Z, et al. Rhamnetin induces apoptosis in human breast cancer cells via the miR-34a/Notch-1 signaling pathway. Oncol Lett (2019) 17(1):676-82.
62. Wang S, Li Z, Liu W, Wei G, Yu N, Ji G. Neohesperidin Induces Cell Cycle Arrest, Apoptosis, and Autophagy via the ROS/JNK Signaling Pathway in Human Osteosarcoma Cells. *The American Journal of Chinese Medicine* (2021) 49(05):1251-74.